Multi-band Gutzwiller wave functions for itinerant ferromagnetism*

Jörg Bünemann and Florian Gebhard
Fachbereich Physik, Philipps-Universität Marburg, D-35032 Marburg, Germany

Werner Weber
Institut für Physik, Universität Dortmund, D-44221 Dortmund, Germany

Multi-band Gutzwiller-correlated wave functions reconcile the contrasting concepts of itinerant band electrons versus electrons localized in partially filled atomic shells. The approximate evaluation of these variational ground states becomes exact in the limit of large coordination number. The result allows the identification of quasi-particle band structures for correlated electron systems. As a first application, we summarize a study of itinerant ferromagnetism in a two-band model, thereby elucidating the co-operation of the Coulomb repulsion and the Hund's-rule exchange. Then, we present results of calculations for ferromagnetic nickel, using a realistic 18 spin-orbital basis of $4s$, $4p$ and $3d$ valence electrons. Good agreement with the experimental ground-state properties of nickel is obtained. In particular, the quasi-particle energy bands agree much better with the photoemission and Fermi surface data than the band structure obtained from spin-density functional theory. Finally, we present results for the variational spinwave dispersion for our two-band model.

I. INTRODUCTION

How well do we understand the itinerant ferromagnetism of iron, nickel, and other transition metals and their compounds?

More than 50 years ago two basically different scenarios had emerged from early quantum-mechanical considerations on electrons in metals with partly filled d bands. In scenario I, suggested by Slater [1] and Stoner [2], band theory alone was proposed to account for itinerant ferromagnetism: due to the Pauli principle, electrons with parallel spins cannot come arbitrarily close to each other ("Pauli" or "exchange hole"), and, thus, a ferromagnetic alignment of the electron spins reduces the total Coulomb energy with respect to the paramagnetic situation ("exchange energy"). This scenario, equivalent to Hartree-Fock theory, was criticized by van Vleck [3]. In an independent-electron theory electrons are distributed statistically over the lattice which implies strong charge fluctuations on the transition metal atoms.

Consequently, as a scenario II, van Vleck [3] emphasized the importance of electron correlations: due to the strong electron-electron interactions, charge fluctuations in the atomic d shells are strongly suppressed ("minimum polarity model"), and, thus, atomic rather than band aspects are decisive for itinerant ferromagnetism. In scenario II, the atomic magnetic moments arise due to the local Coulomb interaction (in particular, Hund's-rule couplings), and they may align because of the electrons' motion through the crystal.

In principle, such a dispute can be resolved in natural sciences. The corresponding theories have to be worked out in detail, and their results and predictions have to be compared to experiments. This was indeed done for scenario I [4]. The (spin-)density functional theory is a refined band theory which describes simple metals with considerable success. Unfortunately, progress for scenario II was much slower. It calls for a theory of correlated electrons, i.e., a genuine many-body problem has to be solved. It was only recently that reliable theoretical tools became available which allow to elucidate scenario II in more detail [5,6,7,8,9].

A first step in this direction was the formulation of appropriate model Hamiltonians which allowed to discuss matters concisely. In 1963/1964 Gutzwiller [10,11], Hubbard [12], and Kanamori [13] independently introduced the Hubbard model which since then has become the standard model for correlated electrons on a lattice. This model covers both aspects of d electrons on a lattice: they can move through the crystal, and they strongly interact when they sit on the same lattice site. The model is discussed in more detail in Sec. II.

Even nowadays, it is impossible to calculate exact ground-state properties of such a model in three dimensions. In 1963/1964 Gutzwiller introduced a trial state to examine variationally the possibility of ferromagnetism in such a model [10,11]. His wave function covers both limits of weak and strong correlations and should, therefore, be suitable to provide qualitative insights into the magnetic phase diagram of the Hubbard model. Gutzwiller-correlated wave functions for multi-band Hubbard models are defined and analyzed in Sec. III.

*Dedicated to Martin C. Gutzwiller on the occasion of his 75th birthday.

As envisaged by van Vleck [3], Gutzwiller [10] found that ferromagnetism is non-generic in the one-band Hubbard model, in contrast to the predictions of the Stoner theory. The reason is simple: the Gutzwiller wave function not only describes the exchange hole between electrons of the same spin species but also the "correlation hole" between electrons of different spin species which forms when the electron-electron interaction is taken into account consistently. Therefore, the energy difference between the correlated paramagnetic and ferromagnetic states is very small, and paramagnetism wins in almost all one-band cases. In the multi-band situation [11], itinerant ferromagnetism is favored by two concomitant effects: (i) the suppression of atomic charge fluctuations such that, (ii), the local exchange interactions give rise to a local magnetic moment as in isolated atoms (Hund's rule). Hence, as proposed by van Vleck, small charge fluctuations *and* local exchange interactions generate large local moments which are present in both the paramagnetic and ferromagnetic phases. At low temperatures the electrons' motion through the crystal may then lead to long-range order of these pre-formed local moments. In this way, Gutzwiller's approach unified and substantiated van Vleck's early ideas on a correlated-electron theory of itinerant ferromagnetism.

Unfortunately, the evaluation of multi-band Gutzwiller wave functions itself poses a most difficult many-body problem. Perturbative treatments [14,15] are constrained to small to moderate interaction strengths. The region of strong correlations could only be addressed within the "Gutzwiller approximation" [10,11,16] and its various extensions [17,18]. Thus, an application to ferromagnetism of real materials was not in sight, and Gutzwiller's qualitative findings were not appreciated much in the sixties.

About 25 years later, a major technical advancement opened a new way to analyze Gutzwiller-correlated wave functions. The one-band Gutzwiller wave function was evaluated exactly in one dimension [19,20], and the Gutzwiller approximation was found to become exact for the one-band Gutzwiller wave function in the limit of infinite spatial dimensions, $d \to \infty$ [19,21,22]. Based on a diagrammatical approach, Gebhard [23] developed a compact formalism which allows to calculate the variational ground-state energy in infinite dimensions without the evaluation of a single diagram. He found that $1/d$ corrections are quantitatively small for the Gutzwiller wave function, i.e., the result in infinite dimensions is a reliable approximation to three dimensions.

Recently, Gebhard's approach was generalized by us to the case of multi-band Gutzwiller wave functions [9]. Thereby, earlier results by Bünemann and Weber [24], based on a generic extension of the Gutzwiller approximation [25], were found to become exact in infinite dimensions [26]. Half a century after van Vleck's call for new many-particle methods and more than thirty years after Gutzwiller's first paper on the subject, techniques are at hand to carry out the program outlined above as scenario II.

Our results on a two-band toy model in Sect. IV confirm Gutzwiller's insights on the fundamental requirements for itinerant ferromagnetism. Substantial atomic Coulomb interactions suppress local charge fluctuations and thereby allow the generation of local moments due to the atomic Hund's-rule exchange couplings. Our quantitative results from a full-scale calculation for nickel in Sect. V confirm these qualitative findings. The quasiparticle properties of this material (e.g., exchange splittings, density of states, topology of the Fermi surface) are reproduced quantitatively from our Gutzwiller-correlated wave functions. In particular, strong electron correlations are required to describe nickel appropriately.

In Sect. VI, we briefly discuss a new method to calculate spinwave spectra of correlated electron systems based on the Gutzwiller variational scheme [27]. In this way, the dispersion relation of the fundamental low-energy excitations can be derived consistently. Albeit the description is based on itinerant electrons, the results for strong ferromagnetism in a generic two-band model resemble those of a Heisenberg model for localized spins. Again, the Gutzwiller approach provides a comprehensive scheme for a unified description of localized and itinerant aspects of transition metals.

In this brief review we skip all technical details and refer the reader to the original literature for further information.

II. HAMILTON OPERATOR

Our multi-band Hubbard model [12] is defined by the Hamiltonian

$$\hat{H} = \sum_{i,j;\sigma,\sigma'} t_{i,j}^{\sigma,\sigma'} \hat{c}_{i;\sigma}^{+} \hat{c}_{j;\sigma'} + \sum_{i} \hat{H}_{i;\mathrm{at}} \equiv \hat{H}_1 + \hat{H}_{\mathrm{at}} \; . \quad (1)$$

Here, $\hat{c}_{i;\sigma}^{+}$ creates an electron with combined spin-orbit index $\boldsymbol{\sigma} = 1, \ldots, 2N$ ($N = 5$ for $3d$ electrons) at the lattice site i of a solid.

The most general case is treated in Ref. [9]. In this work we assume for simplicity that different types of orbitals belong to different representations of the point group of the respective atomic state (e.g., s, p, $d(e_g)$, $d(t_{2g})$). In this case, different types of orbitals do not mix locally, and, thus, the crystal field is of the from $t_{i,i}^{\sigma,\sigma'} = \epsilon_{\sigma} \delta_{\sigma,\sigma'}$. Consequently, we use normalized single-particle product states $|\Phi_0\rangle$ which respect the symmetry of the lattice, i.e.,

$$\langle \Phi_0 | \hat{c}_{i;\sigma}^{+} \hat{c}_{i;\sigma'} | \Phi_0 \rangle = \delta_{\sigma,\sigma'} n_{i;\sigma}^{0} \; . \quad (2)$$

We further assume that the local interaction is site-independent

$$\hat{H}_{i;\mathrm{at}} = \sum_{\sigma_1,\sigma_2,\sigma_3,\sigma_4} \mathcal{U}^{\sigma_1,\sigma_2;\sigma_3,\sigma_4} \hat{c}^+_{i;\sigma_1} \hat{c}^+_{i;\sigma_2} \hat{c}_{i;\sigma_3} \hat{c}_{i;\sigma_4} \ . \quad (3)$$

This term represents all possible local Coulomb interactions.

As our basis for the atomic problem we choose the configuration states

$$\begin{aligned} |I\rangle &= |\boldsymbol{\sigma_1}, \boldsymbol{\sigma_2}, \ldots\rangle \\ &= \hat{c}^+_{i;\sigma_1} \hat{c}^+_{i;\sigma_2} \cdots |\mathrm{vaccum}\rangle \quad (\boldsymbol{\sigma_1} < \boldsymbol{\sigma_2} < \cdots) \ , \end{aligned} \quad (4)$$

which are the "Slater determinants" in atomic physics. The diagonalization of the Hamiltonian $\hat{H}_{i;\mathrm{at}}$ is a standard exercise [28]. The eigenstates $|\Gamma\rangle$ obey

$$|\Gamma\rangle = \sum_I T_{I,\Gamma} |I\rangle \ , \quad (5)$$

where $T_{I,\Gamma}$ are the elements of the unitary matrix which diagonalizes the atomic Hamiltonian matrix with entries $\langle I|\hat{H}_{i;\mathrm{at}}|I'\rangle$. Then,

$$\hat{H}_{i;\mathrm{at}} = \sum_\Gamma E_\Gamma \hat{m}_\Gamma \ , \quad (6)$$

$$\hat{m}_\Gamma = |\Gamma\rangle\langle\Gamma| \ . \quad (7)$$

The atomic properties, i.e., eigenenergies E_Γ, eigenstates $|\Gamma\rangle$, and matrix elements $T_{I,\Gamma}$, are essential ingredients of our solid-state theory.

III. MULTI-BAND GUTZWILLER WAVE FUNCTIONS

Gutzwiller-correlated wave functions are written as a many-particle correlator $\hat{P}_\mathrm{G}$ acting on a normalized single-particle product state $|\Phi_0\rangle$,

$$|\Psi_\mathrm{G}\rangle = \hat{P}_\mathrm{G} |\Phi_0\rangle \ . \quad (8)$$

The single-particle wave function $|\Phi_0\rangle$ contains many configurations which are energetically unfavorable with respect to the atomic interactions. Hence, the correlator $\hat{P}_\mathrm{G}$ is chosen to suppress the weight of these configurations to minimize the total energy in (1). In the limit of strong correlations the Gutzwiller correlator $\hat{P}_\mathrm{G}$ should project onto atomic eigenstates. Therefore, the proper multi-band Gutzwiller wave function with atomic correlations reads

$$\begin{aligned} \hat{P}_\mathrm{G} &= \prod_i \hat{P}_{i;\mathrm{G}} \ , \\ \hat{P}_{i;\mathrm{G}} &= \prod_\Gamma \lambda_{i;\Gamma}^{\hat{m}_{i;\Gamma}} = \prod_\Gamma \left[1 + (\lambda_{i;\Gamma} - 1)\, \hat{m}_{i;\Gamma}\right] \\ &= 1 + \sum_\Gamma (\lambda_{i;\Gamma} - 1)\, \hat{m}_{i;\Gamma} \ . \end{aligned} \quad (9)$$

The 2^{2N} variational parameters $\lambda_{i;\Gamma}$ per site are real, positive numbers. For $\lambda_{i;\Gamma_0} \neq 0$ and all other $\lambda_{i;\Gamma} = 0$ all atomic configurations at site i but $|\Gamma_0\rangle$ are removed from $|\Phi_0\rangle$. Therefore, by construction, $|\Psi_\mathrm{G}\rangle$ covers both limits of weak and strong coupling. In this way it incorporates both itinerant and local aspects of correlated electrons in narrow-band systems.

The class of Gutzwiller-correlated wave functions as specified in (9) was evaluated exactly in the limit of infinite dimensions in Ref. [9]. The expectation value of the Hamiltonian (1) reads

$$\begin{aligned} \langle \hat{H} \rangle &= \frac{\langle \Psi_\mathrm{G} | \hat{H} | \Psi_\mathrm{G} \rangle}{\langle \Psi_\mathrm{G} | \Psi_\mathrm{G} \rangle} \\ &= \sum_{i \neq j;\sigma,\sigma'} t_{i,j}^{\sigma,\sigma'} \sqrt{q_{i;\sigma}} \sqrt{q_{j;\sigma'}} \langle \Phi_0 | \hat{c}^+_{i;\sigma} \hat{c}_{j;\sigma'} | \Phi_0 \rangle \\ &\quad + \sum_{i;\sigma} \epsilon_\sigma n^0_{i;\sigma} + \sum_{i;\Gamma} E_\Gamma m_{i;\Gamma} \ . \end{aligned} \quad (10)$$

Here, $n^0_{i,\sigma} = \langle \Phi_0 | \hat{n}_{i;\sigma} | \Phi_0 \rangle$ is the local particle density in $|\Phi_0\rangle$. The local q-factors are given by [9]

$$\begin{aligned} \sqrt{q_\sigma} = \sqrt{\frac{1}{n^0_\sigma (1 - n^0_\sigma)}} \sum_{\Gamma,\Gamma'} \sqrt{\frac{m_\Gamma m_{\Gamma'}}{m^0_\Gamma m^0_{\Gamma'}}} \sum_{I,I' \ (\sigma \notin I, I')} f^I_\sigma f^{I'}_\sigma \\ \sqrt{m^0_{(I' \cup \sigma)} m^0_{I'}} T^+_{\Gamma,(I \cup \sigma)} T_{(I' \cup \sigma),\Gamma} T^+_{\Gamma',I'} T_{I,\Gamma'} \ , \end{aligned} \quad (11)$$

where $m^0_{i;I}$ ($m^0_{i;\Gamma}$) is the probability to find the configuration $|I\rangle$ (the atomic eigenstate $|\Gamma\rangle$) on site i in the single-particle product state $|\Phi_0\rangle$. The fermionic sign function

$$f^I_\sigma \equiv \langle I \cup \boldsymbol{\sigma} | \hat{c}^+_\sigma | I \rangle \quad (12)$$

gives a minus (plus) sign if it takes an odd (even) number of anticommutations to shift the operator $\hat{c}^+_\sigma$ to its proper place in the sequence of electron creation operators in $|I \cup \boldsymbol{\sigma}\rangle$.

Eqs. (10) and (11) show that we may replace the original variational parameters $\lambda_{i;\Gamma}$ by their physical counterparts, the atomic occupancies $m_{i;\Gamma}$. They are related by the simple equation [9]

$$m_{i;\Gamma} = \lambda^2_{i;\Gamma} m^0_{i;\Gamma} \ . \quad (13)$$

The probability for an empty site ($|I| = 0$) is obtained from the completeness condition,

$$m_{i;\emptyset} = 1 - \sum_{\Gamma \, (|\Gamma| \geq 1)} m_{i;\Gamma} \ . \quad (14)$$

The probabilities for a singly occupied site ($|I| = 1$) are given by

$$m_{i;\sigma} = n^0_{i;\sigma} - \sum_{I \, (|I| \geq 2) \, (\sigma \in I)} m_{i;I} \ , \quad (15a)$$

$$m_{i;I} = \sum_K \left| \sum_\Gamma \sqrt{\frac{m_{i;\Gamma}}{m^0_{i;\Gamma}}} T^+_{\Gamma,I} T_{K,\Gamma} \right|^2 m^0_{i;K} \ . \quad (15b)$$

The parameters $m_{i;\emptyset}$ and $m_{i;\sigma}$ must not be varied independently. All quantities in (10) are now expressed in terms of the atomic multi-particle occupancies $m_{i;\Gamma}$ ($|\Gamma| \geq 2$), the local densities $n^0_{i;\sigma}$, and further variational parameters in $|\Phi_0\rangle$.

It is seen that the variational ground-state energy can be cast into the form of the expectation value of an effective single-particle Hamiltonian with renormalized electron transfer amplitudes $\widetilde{t}^{\sigma,\sigma'}_{i,j}$,

$$\hat{H}_{\rm eff} = \sum_{i\neq j;\sigma,\sigma'} \widetilde{t}^{\sigma,\sigma'}_{i,j}\hat{c}^+_{i;\sigma}\hat{c}_{j;\sigma'} + \sum_{i;\sigma}\epsilon_\sigma \hat{n}_{i;\sigma} + \sum_{i;\Gamma} E_\Gamma m_{i;\Gamma}\,,$$
$$\widetilde{t}^{\sigma,\sigma'}_{i,j} = \sqrt{q_{i;\sigma}}\sqrt{q_{j;\sigma'}}\,t^{\sigma,\sigma'}_{i,j}\,. \qquad (16)$$

Therefore, $|\Phi_0\rangle$ is the ground state of $\hat{H}_{\rm eff}$ whose parameters have to be determined self-consistently from the minimization of $\langle\Phi_0|\hat{H}_{\rm eff}|\Phi_0\rangle$ with respect to $m_{i;\Gamma}$ and $n^0_{i;\sigma}$. For the optimum set of parameters, $\hat{H}^{\rm opt}_{\rm eff}$ *defines* a band structure for *correlated* electrons. Similar to density-functional theory, this interpretation of our ground-state results opens the way to detailed comparisons with experimental results.

Applications are discussed in the next two sections.

IV. RESULTS FOR A GENERIC TWO-BAND MODEL

The atomic Hamiltonian for a two-band model ($b = 1, 2$) can be cast into the form

$$\hat{H}_{i;\rm at} = U\sum_b \hat{n}_{b,\uparrow}\hat{n}_{b,\downarrow} + U'\sum_{\sigma,\sigma'}\hat{n}_{1,\sigma}\hat{n}_{2,\sigma'} - J\sum_\sigma \hat{n}_{1,\sigma}\hat{n}_{2,\sigma}$$
$$+J\sum_\sigma \hat{c}^+_{1,\sigma}\hat{c}^+_{2,-\sigma}\hat{c}_{1,-\sigma}\hat{c}_{2,\sigma} \qquad (17)$$
$$+J_{\rm C}\left(\hat{c}^+_{1,\uparrow}\hat{c}^+_{1,\downarrow}\hat{c}_{2,\downarrow}\hat{c}_{2,\uparrow} + \hat{c}^+_{2,\uparrow}\hat{c}^+_{2,\downarrow}\hat{c}_{1,\downarrow}\hat{c}_{1,\uparrow}\right).$$

For two orbitals, $\hat{H}_{\rm at}$ exhausts all possible two-body interaction terms.

We assume that the model describes two degenerate $d(e_g)$ orbitals which leads to the following restrictions enforced by the cubic symmetry [28]: (i) $J = J_{\rm C}$, and (ii) $U - U' = 2J$. Therefore, there are two independent Coulomb parameters, the local Coulomb repulsion U and the local exchange coupling J. Since $U, U' = \mathcal{O}(10\,{\rm eV})$ are of the same order of magnitude the relation (ii) shows that $J = \mathcal{O}(1\,{\rm eV})$ is of the typical strength of the atomic Hund's rule couplings.

For the one-particle part $\hat{H}_1$ we use an orthogonal tight-binding Hamiltonian with first and second nearest neighbor hopping matrix elements. We apply the two-center approximation for the hopping matrix elements and exclude any spin-flip hopping. The resulting band structure (width $W = 6.6\,{\rm eV}$) is discussed in detail in Ref. [9].

In the following we concentrate on two band-fillings $0 \leq n \leq 4$, the number of electrons per lattice site. Alternatively, we use $0 \leq n_\sigma = n/4 \leq 1$, the particle density per band and per spin direction. For $n_\sigma = 0.29$, the non-interacting density of states has a maximum which is most favorable for ferromagnetism according to the Stoner (i.e, Hartree-Fock) theory. Moreover, we study $n_\sigma = 0.35$, where the density-of-states has a positive curvature.

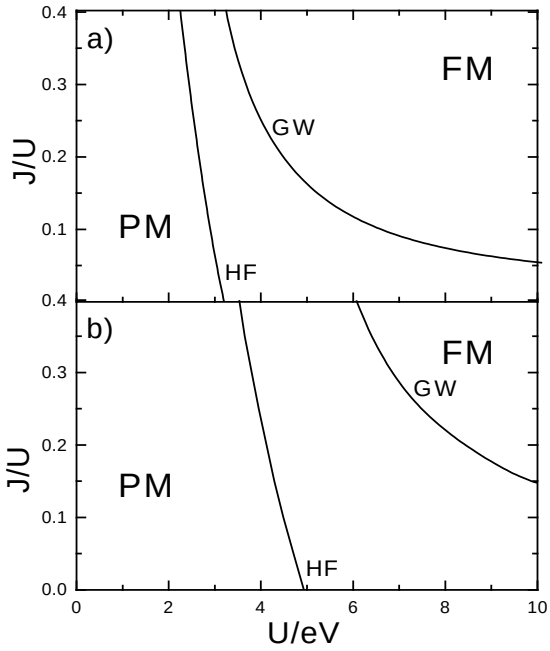

FIG. 1. Phase diagram as a function of U and J for the Hartree-Fock–Stoner theory (HF) and the Gutzwiller wave function (GW) for (a) $n/4 = 0.29$ and (b) $n/4 = 0.35$; PM: paramagnet, FM: ferromagnet.

In Fig. 1 we display the J-U phase diagram for both fillings. It shows that Hartree–Fock theory always predicts a ferromagnetic instability. In contrast, the correlated-electron approach strongly supports the ideas of van Vleck [3] and Gutzwiller [11]: (i) a substantial on-site exchange J is required for the occurrence of ferromagnetism if, (ii), realistic Coulomb repulsions U are assumed. In 1964 Gutzwiller wrote "*... one may hope to show some day that the terms (ii) can never induce ferromagnetism at all by themselves ...*". Fig. 1 strongly supports Gutzwiller's ideas on the importance of the local Hund's-rule couplings. At the same time the comparison of Figs. 1a and 1b shows the importance of band-structure effects which are the basis of the Stoner theory. The ferromagnetic phase in the U-J phase diagram is much bigger when the density of states at the Fermi energy is large. Therefore, the Stoner mechanism for ferromagnetism is well taken into account by Gutzwiller's correlated-electron approach.

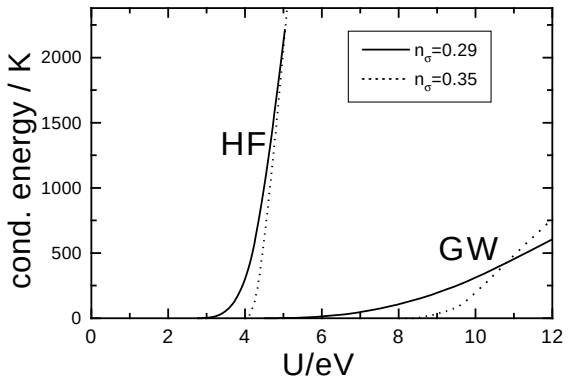

FIG. 2. Condensation energy as a function of U for $J = 0.2U$ for the Hartree–Fock theory (HF) and the Gutzwiller wave function (GW) for $n/4 = 0.29$ (full lines) and $n/4 = 0.35$ (dashed lines).

In Fig. 2, we display the energy differences between the paramagnetic and ferromagnetic ground states ("condensation energy", $E_{\rm cond}$) as a function of the interaction strength for $J = 0.2U$. This quantity should be of the order of the Curie temperature which is in the range of $100\,{\rm K} - 1000\,{\rm K}$ in real materials. The Hartree-Fock–Stoner theory yields such small condensation energies only in the range of $U \approx 4\,{\rm eV}$; for larger U, $E_{\rm cond}$ is of order U. In any case, the interaction parameter U has to be tuned very precisely to give condensation energies which concur with experimental Curie temperatures [1]. In contrast, for the Gutzwiller-correlated wave function, we find relatively small condensation energies $E_{\rm cond} = 0.5 \cdot 10^3\,{\rm K}$ even for interaction values as large as twice the bandwidth ($U \approx 12\,{\rm eV}$). Moreover, the dependence of the condensation energy on U is rather weak such that uncertainties in U do not drastically influence the estimates for the Curie temperature.

These toy-model studies show that the Gutzwiller variational approach contains all the fundamental elements for a successful theory of itinerant ferromagnetism. In the next section we show how to quantify this statement for ferromagnetic nickel.

V. CORRELATED BAND-STRUCTURE OF NICKEL

A. Discrepancies between experiment and SDFT

Of all the iron group magnetic metals, nickel is the most celebrated case of discrepancies between the results from experiment and from SDFT. From very early on, the photo-emission data have indicated that the width of the occupied part of the d bands is approximately $W^*_{\rm occ} = 3.3\,{\rm eV}$ [29] whereas all SDFT results yield values of $W^*_{\rm occ,\,SDFT} = 4.5\,{\rm eV}$ or larger [4,29]. Similarly, the low temperature specific heat data [30] give a much larger value of $N^*(E_{\rm F})$, the quasi-particle density of states at the Fermi energy (3.0 versus 1.9 states/(eV atom)), which indicates a quasi-particle mass enhancement by a factor of approximately 1.6. Here, the Sommerfeld formula is used to convert the specific heat data; the theoretical value follows directly from the quasi-particle band structure. Furthermore, very detailed photo-emission studies at symmetry points and along symmetry lines of the Brillouin zone show discrepancies to SDFT results for individual band-state energies which are of similar magnitude as seen in the overall d bandwidth.

The studies also revealed even bigger discrepancies in the exchange splittings of majority spin and minority spin bands. The SDFT results give a rather isotropic exchange splitting of about 600 meV [4,29,31]. In contrast, the photo-emission data show small and highly anisotropic exchange splittings between 160 meV for pure $d(e_g)$ states such as X_2 and 330 meV for pure $d(t_{2g})$ states, the latter value estimated from the exchange splitting of Λ_3 states along Γ to L [32,33]. The much larger and much too isotropic exchange splitting of the SDFT results has further consequences.

1. The experimental magnetic moment of the strong ferromagnet Ni is $\mu = 0.61\mu_{\rm B}$; yet of relevance is its spin-only part $\mu_{\text{spin-only}} = 0.55\mu_{\rm B}$ [34]. The SDFT result is $\mu_{\text{spin-only}} = 0.59\mu_{\rm B}$ [4], an overestimate related to the too large exchange splitting.
2. the X_2 state of the minority spin bands lies below $E_{\rm F}$ [35], whereas all SDFT results predict it to lie above the Fermi level [4,36,37]. As a consequence, the SDFT Fermi surface exhibits *two* hole ellipsoids around the X point of the Brillouin zone while in the de-Haas–van-Alphen experiments only *one* ellipsoid has been found [36,38].
3. The strong t_{2g}-e_g anisotropy is also reflected in the total d hole spin density, i.e., in the observation that the d-hole part of the Ni magnetic moment has 81% $d(t_{2g})$ and 19% $d(e_g)$ character [34], while the SDFT results give a ratio of 74% to 26% [39].

In the late 70's and early 80's various authors have investigated in how far many-body effects improve the agreement between theory and experiment, see, e.g., Refs. [40,41]. For example, Cooke et al. [40] introduced an anisotropic exchange splitting as a fit parameter.

B. Parameterization and minimization

For the single-particle Hamiltonian $\hat{H}_1$ in (1) we use a nine-orbital s, p, d basis. The hopping matrix elements $t_{i,j}^{\sigma,\sigma'}$ are determined from a least-square fit to energy bands obtained from a density-functional-theory calculation for non-magnetic nickel. The root-mean-square deviation of the d-band energies is about 5 meV. Details of this calculation will be published elsewhere [42].

The atomic Hamiltonian $\hat{H}_{\rm at}$ in (3) is restricted to only d orbitals. As a consequence, there are three independent interaction parameters (we use the spherical-atom approximation), which can be expressed either as Slater integrals F^k ($k = 0, 2, 4$) or as Racah parameters A, B, C [28]. We neglect any cubic crystal-field corrections to the interaction parameters and, furthermore, put $C/B = 4.5$, as suggested by the results of ligand-field theory [28]. We find that $A \approx 10\,\mathrm{eV}$ and $C \approx 0.1\,\mathrm{eV}$ are the choice which best reproduces the experimental results; see below.

The number of multi-electron states $|\Gamma\rangle$ is $2^{10} - 11$; because of the cubic site symmetry, the number of independent (internal) variational parameters m_Γ reduces to approximately 200 for paramagnetic and to approximately 400 for ferromagnetic solutions. For the magnetic solutions, there exist a certain number of (external) variational parameters Δ_α in the one-particle wave function $|\Phi_0\rangle$. In particular, the Δ_α influence the spin-orbital densities $n^0_{i;b,\sigma}$ ($b = d, p, s$). Among the Δ_α are the "exchange splittings" of the individual orbitals (b, σ) and $(b, -\sigma)$, i.e., these parameters determine the degree of magnetization in $|\Phi_0\rangle$. Most important are the exchange splittings for $d(e_g)$ and $d(t_{2g})$ orbitals, of minor importance are those for s and p orbitals. Furthermore, the $d(e_g)$ vs. $d(t_{2g})$ crystal-field splitting has to be included in the set of Δ_α. Technically, each $|\Phi_0\rangle$, which is a functional of the external variational parameters Δ_α, defines a band structure and, consequently, a Fermi surface. Therefore, calculating the particle densities $n^0_{i;b,\sigma}$ and the expectation values $\langle\Phi_0|\hat{H}_{\rm eff}|\Phi_0\rangle$ implies momentum-space integrations up to the respective Fermi surface. It should be noted that the introduction of the variational parameters Δ_α causes a charge flow between the d, and s and p states which has to be compensated by using appropriate "chemical potentials".

The optimum $|\Phi_0\rangle$ for a given set of $\{\Delta_\alpha\}$, $|\Phi_0^{\rm opt}\rangle_\alpha$ is the ground state of the effective single-particle Hamiltonian (16) with renormalized hopping matrix elements $\widetilde{t}_{i,j}$ which, through the q factors, are functions of the internal variational parameters m_Γ. Thus, $|\Phi_0^{\rm opt}\rangle_\alpha$ can be obtained from a self-consistent procedure, starting with $q_\sigma = 1$, i.e., with $|\Phi_0^{\rm bare}\rangle_\alpha$. After minimization of the internal variational parameters, the resulting values for q_σ define a new effective Hamiltonian from which a new $|\Phi_0\rangle_\alpha$ is constructed. In this step, the Fermi surface integrations have to be repeated. Self-consistency is usually reached rather quickly, i.e., $|\Phi_0^{\rm opt}\rangle_\alpha$ is found after three to five iterations.

The global minimum, $|\Phi_0^{\rm opt}\rangle_{\rm global}$ is found by a search through the N_α-dimensional space of the external variational parameters Δ_α. This search can be sped up by first optimizing with respect to the most important external variational parameter which is the isotropic exchange splitting Δ_d. In a second step, the anisotropy of the exchange splitting is investigated, i.e., we introduce Δ_{e_g} and $\Delta_{t_{2g}}$, keeping the average Δ_d close to the value of $\Delta_d^{\rm opt}$. The searches for $\Delta_d^{\rm opt}$ and for $\Delta_{e_g}^{\rm opt}$ and $\Delta_{t_{2g}}^{\rm opt}$ can be carried out starting with $|\Phi_0^{\rm bare}\rangle$. Only then the self-consistency procedure for $|\Phi_0^{\rm opt}\rangle$ has to be launched.

Typical energy gains are (in meV):

$$E_0^{\rm bare} - E_0^{\rm bare}(\Delta_d^{\rm opt}) \approx 10 - 100, \quad \text{(18a)}$$

$$E_0^{\rm bare}(\Delta_d^{\rm opt}) - E_0^{\rm bare}(\Delta_{e_g}^{\rm opt}, \Delta_{t_{2g}}^{\rm opt}) \approx 5 - 10, \quad \text{(18b)}$$

$$E_0^{\rm bare}(\Delta_{e_g}^{\rm opt}, \Delta_{t_{2g}}^{\rm opt}) - E_0^{\rm opt}(\Delta_{e_g}^{\rm opt}, \Delta_{t_{2g}}^{\rm opt}) \approx 5 - 10. \quad \text{(18c)}$$

The energy gains from the variations of Δ_s and Δ_p are of the order of 0.1 meV.

At present, our description does not contain the spin-orbit coupling which could be relevant in some transition metals. This interaction contributes to the orbital moment $\mu_{\rm orbit} = 0.06\mu_{\rm B}$ to the total magnetic moment. The inclusion of the spin-orbit coupling poses no principle difficulties [9] but it considerably enhances the numerical complexity of the problem. Moreover, we may want to extend our basis set beyond the nine bands $4s$, $4p$, and $3d$ to allow for a further relaxation of the one-particle wave functions. Again, this is feasible but numerically much more costly. Lastly, one may want to include some atomic p-p and p-d interactions. All these extensions are left for future studies.

C. Comparison to experiments

Typical results of our calculations for Ni are summarized in table I. They are obtained from the multi-band Gutzwiller method utilizing the nine-orbital tight-binding model based on DFT energy band calculations for non-magnetic Ni, and employing values of $A = 10\,\mathrm{eV}$ and $C = 0.1\,\mathrm{eV}$, with $C/B = 4.5$.

The width of the d bands is predominantly determined by A (essentially the Hubbard-U), via the values of the hopping reduction factors $q_{b,\sigma}$. The exchange splittings and, consequently, the magnetic moment are strongly influenced by C and only moderately by A. The Racah parameter C causes the Hund's-rule splitting of the d^8 multiplets; in the hole picture, d^8 is the only many-particle configuration which is significantly occupied (by 1.90 electrons), while 5.94 electrons are in d^9, 0.89 electrons are in d^{10}, and 1.18 electrons have s or p character.

Generally, the Gutzwiller results agree much better with experiment than the SDFT results. This is the case for, (i), the d bandwidth W^*, (ii), the value for $N^*(E_{\rm F})$, (iii), the positions of individual quasi-particle energies, (iv), the values of the exchange splittings, (v), their t_{2g}-e_g anisotropy, and, (vi), the t_{2g}/e_g ratio of the d part of the magnetic moment. As a consequence of the small $d(e_g)$ exchange splitting, the $X_{2\downarrow}$ state lies *below* $E_{\rm F}$ and, thus, the Fermi surface exhibits only *one* hole ellipsoid around X, in nice agreement with experiment.

	Exp.	Ref.	this work	SDFT
$\mu_{\text{spin-only}}/\mu_{\text{B}}$	0.55	[34]	0.53	0.59
$r(t_{2g}/e_g)$	4.3	[34]	5.1	2.8
$W^*_{\text{occ}} = -\langle X_1\rangle$/eV	-3.3 ± 0.2	[29]	-3.14	-4.86
W^*/eV	3.5 ± 0.3	[29]	3.29	5.20
$N^*(E_{\text{F}})$/(eV atom)	3.0	[30]	2.6	1.9
$\langle X_3\rangle$/eV	-2.8 ± 0.2	[29]	-2.94	-4.06
$X_{2\uparrow}$/eV	-0.24 ± 0.02	[43,35]	-0.22	-0.56
$X_{2\downarrow}$/eV	-0.06 ± 0.02	[43,35]	-0.04	$+0.09$
$X_{5\uparrow}$/eV	-0.10 ± 0.02	[43,44]	-0.14	-0.22
$X_{5\downarrow}$/eV	0.23 ± 0.04	[43,44]	0.25	0.34
$\langle\Gamma_{12}\rangle$/eV	-0.4 ± 0.1	[29]	-0.64	-1.02
$\langle\Gamma_{25'}\rangle$/eV	-1.1 ± 0.2	[29]	-1.45	-2.14
$\langle L_3\rangle$/eV	-1.3 ± 0.1	[29]	-1.49	-2.23
$\Delta((1/2)\Gamma L)$/eV	0.21 ± 0.02	[33]	0.30	0.60

TABLE I. Comparison of experimental and theoretical results. Parameters for the present work are: $A = 10\,\text{eV}$, $C = 0.1\,\text{eV}$, and $C/B = 4.5$. The SDFT results are quoted from Ref. [4]; the result for $r(t_{2g}/e_g)$ is taken from Ref. [39]. $\mu_{\text{spin-only}}$: spin contribution to the magnetic moment; $r(t_{2g}/e_g)$: ratio between t_{2g} and e_g contribution to the magnetic moment $\mu_{\text{spin-only}}$; $W^* = X_{5\downarrow} - \langle X_1\rangle$: quasi-particle bandwidth; W^*_{occ}: occupied quasi-particle bandwidth; $N^*(E_{\text{F}})$: quasi-particle density of states at E_{F}; $\langle\ldots\rangle$/eV: spin-averaged energies of the quasi-particle states at various high-symmetry points of the Brillouin zone; $X_{2,5\,\sigma}$: energies of the spin-σ quasi-particle bands with respective symmetries X_2/X_5 at the X point; $\Delta((1/2)\Gamma L)$: typical exchange splitting of the highest-lying Λ_3 quasi-particle states halfway between Γ and L.

The large anisotropy of the exchange splittings is a result of our ground-state energy optimization, which allows $\Delta_{t_{2g}}$ and Δ_{e_g} to be independent variational parameters. We find $\Delta_{t_{2g}} \approx 3\Delta_{e_g} \approx 800\,\text{meV}$. Note that these values enter $|\Phi_0^{\text{bare}}\rangle$ and are renormalized by factors $q_{b,\uparrow} \approx 0.7$, $q_{b,\downarrow} \approx 0.6$, when $|\Phi_0^{\text{opt}}\rangle$ is reached. This also implies that the width of the majority spin bands is about 10% bigger than that of the (higher lying) minority spin bands. It causes a further reduction of the exchange splittings of states near E_{F}, especially for those with strong t_{2g} character. Note that this band dispersion effect causes larger exchange splittings near the bottom of the d bands, e.g., 0.45 eV splitting of X_1 and 0.74 eV splitting of X_3. There, however, the quasi-particle linewidths have increased to 1.25 eV and 1.4 eV, respectively [29], so that an exchange splitting near the bottom of the d bands could, so far, not be observed experimentally. When we investigate the quasi-particle energies in the middle of the d bands, such as Γ_{12}, $\Gamma_{25'}$, or L_3, we observe that our theoretical values lie consistently below the experimental ones. If we assume that these states can be measured more reliably than those near the bottom of the d band, we may conclude that the value of A could still be somewhat bigger than 10 eV. Studies with larger A values are presently carried out.

We think that the large anisotropy originates from peculiarities special to Ni with its almost completely filled d bands and its fcc lattice structure. Near the top of the d bands, the t_{2g} states dominate because they exhibit the biggest hopping integrals to nearest neighbors, $t^{(1)}_{dd\sigma} \approx 0.5\,\text{eV}$. The e_g states have $t^{(1)}_{dd\pi} \approx -0.3\,\text{eV}$ to nearest neighbors, and $t^{(2)}_{dd\sigma} \approx 0.1\,\text{eV}$ to next-nearest neighbors; the latter are small because of the large lattice distance to second neighbors. The e_g states also mix with the nearest-neighbor t_{2g} states with $t^{(1)}_{dd\pi}$-type coupling. Therefore, the system can gain more band energy by avoiding occupation of anti-bonding t_{2g} states in the minority spin bands via large values of $\Delta_{t_{2g}}$, at the expense of allowing occupation of less anti-bonding e_g states via small Δ_{e_g} values. Note that this scenario is special to nickel and should not apply to materials with a bcc lattice structure which have almost equal nearest and next-nearest neighbor separations. Since the bands in nickel are almost completely filled, the suppression of charge fluctuations actually reduces the number of atomic configurations where the Hund's-rule coupling is active. It is also in this respect that nickel does not quite reflect the generic situation of other transition metals with less completely filled d bands; see Sect. IV.

The agreement between theory and experiments on nickel shows that our multi-band Gutzwiller theory is a useful tool for the theoretical description of the ground-state properties of transition metals and their compounds. In the next section we describe a way to calculate consistently low-energy excitations in itinerant ferromagnets within our variational approach.

VI. SPINWAVES IN ITINERANT FERROMAGNETS

As in magnetic insulators, the elementary excitations in itinerant ferromagnets are spinwaves. Since ground-state properties are well described by Gutzwiller-correlated wave functions it is highly desirable to derive spinwave dispersions from the same variational approach.

In fact, the variational principle can also be used to calculate excited states [45]. If $|\Phi\rangle$ is the ferromagnetic, exact ground state with energy E_0, the trial states

$$|\Psi(q)\rangle = \hat{S}^-_q|\Phi\rangle \tag{19}$$

are necessarily orthogonal to $|\Phi\rangle$, and provide an exact upper bound to the first excited state with momentum q and energy $\epsilon(q)$

$$\epsilon(q) \le E_{\text{s}}(q) \equiv \frac{\langle\Psi(q)|\hat{H}|\Psi(q)\rangle}{\langle\Psi(q)|\Psi(q)\rangle} - E_0\ . \tag{20}$$

Here, $\hat{S}^-_q = (\hat{S}^+_q)^+ = \sum_{l,b}\exp(-iql)\hat{c}^+_{l,b,\downarrow}\hat{c}_{l,b,\uparrow}$ flips a spin from up to down in the system whereby it changes the total momentum of the system by q. In this way, the

famous Bijl-Feynman formula for the phonon-roton dispersion in superfluid Helium was derived [46]. In the case of ferromagnetism the excitation energies $E_{\rm s}(q)$ can be identified with the spinwave dispersion if a well-defined spinwave exists at all [27]. Experimentally this criterion is fulfilled for small momenta q and energies $E_{\rm s}(q)$.

Unfortunately, we do not know the exact ground state or its energy in general. However, we may hope that the Gutzwiller wave function $|\Psi_{\rm G}\rangle$ is a good approximation to the true ground state. Then, the states

$$|\Psi_{\rm G}(q)\rangle = \hat{S}_q^- |\Psi_{\rm G}\rangle \tag{21}$$

will provide a reliable estimate for $E_{\rm s}(q)$,

$$E_{\rm s}(q) \approx E_{\rm s}^{\rm var}(q) = \frac{\langle\Psi_{\rm G}|\hat{S}_q^+ \hat{H} \hat{S}_q^-|\Psi_{\rm G}\rangle}{\langle\Psi_{\rm G}|\hat{S}_q^+ \hat{S}_q^-|\Psi_{\rm G}\rangle} - \frac{\langle\Psi_{\rm G}|\hat{H}|\Psi_{\rm G}\rangle}{\langle\Psi_{\rm G}|\Psi_{\rm G}\rangle} \ . \tag{22}$$

Naturally, $E_{\rm s}^{\rm var}(q)$ does not obey any strict upper-bound principles.

The Hamiltonian (1) commutes with the operator for the total spin. Thus, for $q = 0$, $\hat{S}_{q=0}^-$ generates a state from the same spin multiplet. Therefore, the spinwave at zero momentum is the Goldstone mode of the ferromagnetic system, $E_{\rm s}(q = 0) = 0$. Within the variational approach $E_{\rm s}^{\rm var}(q = 0) = 0$ is guaranteed if we choose $|\Psi_{\rm G}\rangle$ as an eigenstate of the total spin operator. This is most easily accomplished by a minor restriction of the variational space for the atomic occupancies [27] with negligible influence on the variational ground-state properties.

The actual calculation of the variational spinwave dispersion is rather involved even in the limit of large dimensions. We note, however, that explicit formulae are available [27] which can directly be applied once the variational parameters have been determined from the minimization of the variational ground-state energy. As a first application, we present results for the two-band toy-model of Sect. IV.

In Fig. 3 we show the variational spinwave dispersion in x direction, $E_{\rm s}^{\rm var}((q_x, 0, 0))$, for the model parameters $n_\sigma = 0.29$, $J = 0.2U$, and the four different values $U/{\rm eV} = 7.8, 10, 12, 13.6$ which correspond to a magnetization per band of $m = 0.12, 0.20, 0.26, 0.28$. This quantity is defined as $0 \le m = (n_{b,\uparrow} - n_{b,\downarrow})/2 \le n/4$. Note that our last case corresponds to an almost complete ferromagnetic polarization. The data fit very well the formula

$$E_{\rm s}^{\rm var}((q_x, 0, 0)) = D q_x^2 (1 + \beta q_x^2) + \mathcal{O}(q_x^6) \ , \tag{23}$$

in qualitative agreement with experiments on nickel [47]. The corresponding values $D = 1.4\,{\rm eV}\mathring{A}^2$ and $D = 1.2\,{\rm eV}\mathring{A}^2$ for $m = 0.26$ and $m = 0.28$, respectively, are of the right order of magnitude for nickel where $D = 0.43\,{\rm eV}\mathring{A}^2$. As lattice constant of our simple-cubic lattice we chose $a = 2.5\mathring{A}$.

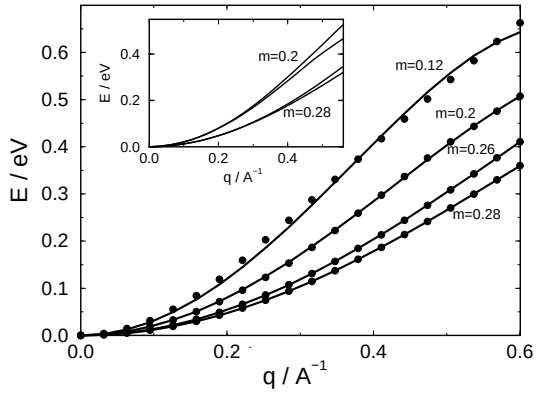

FIG. 3. Variational spinwave dispersion in x direction, $E_{\rm s}^{\rm var}((q_x, 0, 0))$, for the two-band model defined in Sect. IV; $n/4 = 0.29$, $J = 0.2U$, and the values $U/{\rm eV} = 7.8, 10, 12, 13.6$ correspond to $m = 0.12, 0.20, 0.26, 0.28$. The lattice constant is $a = 2.5\mathring{A}$. Inset: $E_{\rm s}^{\rm var}((q_x, 0, 0))$ and $E_{\rm s}^{\rm var}((q_x, q_x, 0))$ for $m = 0.2$ and $m = 0.28$, respectively. The spinwave dispersion is almost isotropic.

As shown in the inset of Fig. 3, the dispersion relation is almost isotropic for q_x values up to half the Brillouin zone boundary [27], in particular for large magnetizations. This is in contrast to the strong dependence of the electron-transfer amplitudes $t_{i,j}$ on the lattice direction. This implies for *strong* ferromagnets that the collective motion of the local moments is similar to that of *localized* spins in an *insulator* [48]. Such ferromagnetic insulators are conveniently described by the Heisenberg model with exchange-interaction between neighboring sites $\langle i, j\rangle$ on a cubic lattice,

$$\hat{H}_{\rm S} = -J \sum_{\langle i,j\rangle} \hat{\vec{S}}_i \hat{\vec{S}}_j \ . \tag{24}$$

For such a model one finds $D = 2SJa^2$. The length of the effective local spins can be calculated from $|\Psi_{\rm G}\rangle$ as $S(S+1) \approx 0.95$ ($S = 0.6$) for $m \ge 0.20$ [9]. Therefore, $J \approx D/(1.2a^2)$, which gives the typical value $J = 0.17\,{\rm eV}$. For an estimate of the Curie temperature $T_{\rm C}$ we use the result from quantum Monte-Carlo calculations [49]

$$T_{\rm C} = 1.44 J S^2 \tag{25}$$

for spins S on a simple-cubic lattice. In this way we find $T_{\rm C} \approx 0.5J = 0.09\,{\rm eV} = 1 \cdot 10^3\,{\rm K}$. This is the same order of magnitude as the condensation energy for these values of the interaction, $E_{\rm cond} = 5 \cdot 10^2\,K$, see Sect. IV. Given the arbitrariness in the relation between $E_{\rm cond}$ and $T_{\rm C}$, and the application of the Heisenberg model to our itinerant-electron system, we may certainly allow for difference of a factor two in these quantities. Nevertheless, the results of this section clearly show that, (i), $E_{\rm cond}$ gives the right order of magnitude for $T_{\rm C}$, and that, (ii), the spinwave dispersion of *strong itinerant* ferromagnets resemble the physics of *localized* spins.

VII. CONCLUSIONS

Which scenario for itinerant ferromagnetism in transition metals is the correct one?

For a long time this questions could not be answered conclusively. Band theory along the lines of Slater and Stoner could be worked out in much detail whereas a correlated-electron description of narrow-band systems was lacking until recently. In fact, van Vleck stated in the summary to his conference contribution in 1953: "The gist of this paper is that it would be highly desirable if good methods of computing with (c) (minimum polarity model) could be developed." In 1963, Gutzwiller laid the foundations for a concise treatment of the problem, and today we are able to draw definite conclusions based on Gutzwiller-correlated multi-band wave functions.

Our results for nickel indicate that the van-Vleck–Gutzwiller scenario is valid. Band theory does not appreciate the strong electronic correlations present in the material which lead to the observed renormalization of the effective mass, exchange splittings, bandwidths, and Fermi surface topology. Moreover, as also covered by our approach, charge fluctuations are small, and large local moments are present both in the paramagnetic and the ferromagnetic phases. Roughly we may say that the electrons' motion through the crystal leads to a ferromagnetic coupling of pre-formed moments which eventually order at low enough temperatures. In this way, strong itinerant ferromagnets resemble ferromagnetic insulators as far as their low-energy properties are concerned: spin-waves exist which destroy the magnetic long-range order at the Curie temperature.

It is thus seen that today computational difficulties no longer obscure "the recognition in principle of the situation which confirms closest to physical reality"(van Vleck, 1953 [3]): transition metals and their compounds are strongly correlated electron systems. More than thirty-five years after their introduction by Gutzwiller [10], our studies clearly show that Gutzwiller-correlated multi-band wave functions successfully describe the low-energy physics of these materials.

ACKNOWLEDGMENTS

We gratefully acknowledge helpful discussions with P. van Dongen, H. Eschrig, and D. Vollhardt. This project is supported in part by the Deutsche Forschungsgemeinschaft under WE 1412/8-1.

[1] J.C. Slater, Phys. Rev. **49**, 537 (1936); *ibid.*, 931 (1936).

[2] E.C. Stoner, Proc. Roy. Soc. A **165**, 372 (1938); for early reviews, see J.C. Slater, Rev. Mod. Phys. **25**, 199 (1953) and E.P. Wohlfarth, *ibid.*, 211 (1953).

[3] J.H. van Vleck, Rev. Mod. Phys. **25**, 220 (1953).

[4] V.L. Moruzzi, J.F. Janak, and A.R. Williams, *Calculated Electronic Properties of Metals* (Pergamon Press, New York, 1978).

[5] W. Nolting, W. Borgieł, V. Dose, and Th. Fauster, Phys. Rev. B **40**, 5015 (1989); W. Borgieł and W. Nolting, Z. Phys. B **78**, 241 (1990).

[6] H. Hasegawa, J. Phys. Soc. Jpn **66**, 3522 (1997); Phys. Rev. B **56**, 1196 (1997); R. Frésard and G. Kotliar, Phys. Rev. B **56**, 12909 (1997).

[7] Th. Obermeier, Th. Pruschke, and J. Keller, Phys. Rev. B **56**, 8479 (1997); Th. Maier, M.B. Zölfl, Th. Pruschke, and J. Keller, Euro. Phys. J. B **7**, 377 (1999); M.B. Zölfl, Th. Pruschke, J. Keller, A.I. Poteryaev, I.A. Nekrasov, and V.I. Anisimov, Phys. Rev. B **61**, 12810 (2000).

[8] D. Vollhardt, N. Blümer, K. Held, M. Kollar, J. Schlipf, M. Ulmke, and J. Wahle, Adv. in Solid-State Phys. **38**, 383 (1999); I.A. Nekrasov, K. Held, N. Blümer, A.I. Poteryaev, V.I. Anisimov, D. Vollhardt, preprint cond-mat/0005207 (2000).

[9] J. Bünemann, W. Weber, and F. Gebhard, Phys. Rev. B **57**, 6896 (1998).

[10] M.C. Gutzwiller, Phys. Rev. Lett. **10**, 159 (1963).

[11] M.C. Gutzwiller, Phys. Rev. **134**, A923 (1964); *ibid.* **137**, A1726 (1965).

[12] J. Hubbard, Proc. Roy. Soc. London Ser. A **276**, 238 (1963); *ibid.* **277**, 237 (1964).

[13] J. Kanamori, Prog. Theor. Phys. **30**, 275 (1963).

[14] G. Stollhoff and P. Fulde, J. Chem. Phys. **73**, 4548 (1980); G. Stollhoff and P. Thalmeier, Z. Phys. B **43**, 13 (1981); A.M. Oleś and G. Stollhoff, Phys. Rev. B **29**, 314 (1984); for further details on the "local ansatz" technique, see P. Fulde, *Electron Correlations in Molecules and Solids*, Springer Series in Solid-State Sciences **100** (Springer, Berlin, 1991).

[15] D. Baeriswyl and K. Maki, Phys. Rev. B **31**, 6633 (1985); D. Baeriswyl, J. Carmelo, and K. Maki, Synth. Met. **21**, 271 (1987).

[16] D. Vollhardt, Rev. Mod. Phys. **56**, 99 (1984).

[17] K.A. Chao and M.C. Gutzwiller J. Appl. Phys. **42** 1420 (1971); K.A. Chao, Phys. Rev. B **4** 4034 (1971); *ibid.* 1088 (1973); J. Phys. C **7** 127 (1974).

[18] P. Fazekas, *Lecture Notes on Electron Correlation and Magnetism*, Series in Mod. Cond. Matt. Phys. **5** (World Scientific, Singapore, 1999), gives an introduction to the theory of ferromagnetism, and a concise description and some applications of the Gutzwiller approximation.

[19] W. Metzner and D. Vollhardt, Phys. Rev. Lett. **59**, 121 (1987); Phys. Rev. B **37**, 7382 (1988).

[20] F. Gebhard and D. Vollhardt, Phys. Rev. Lett. **59**, 1472 (1987); Phys. Rev. B **38**, 6911 (1988).

[21] W. Metzner and D. Vollhardt, Phys. Rev. Lett. **62**, 324 (1989).

[22] For a review, see F. Gebhard, *The Mott Metal-Insulator Transition* (Springer, Berlin, 1997).

[23] F. Gebhard, Phys. Rev. B **41**, 9452 (1990).

[24] J. Bünemann and W. Weber, Phys. Rev. B **55**, 4011 (1997).

[25] J. Bünemann, Eur. Phys. J. B **4**, 29 (1998).

[26] J. Bünemann, F. Gebhard, and W. Weber, J. Phys. Cond. Matt. **8**, 7343 (1997).
[27] J. Bünemann, preprint cond-mat/0005154 (2000).
[28] S. Sugano, Y. Tanabe, and H. Kamimura, *Multiplets of Transition-Metal Ions in Crystals*, Pure and Applied Physics **33** (Academic Press, New York, 1970).
[29] W. Eberhardt and E.W. Plummer, Phys. Rev. B **21**, 3245 (1980).
[30] M. Dixon, F.E. Hoare, T.M. Holden, and D.E. Moody, Proc. R. Soc. A **285**, 561 (1965).
[31] J. Callaway in *Physics of Transition Metals*, ed. by P. Rhodes (Conf. Ser. Notes **55**, Inst. of Physics, Bristol, 1981), p. 1.
[32] M. Donath, Surface Science Reports **20**, 251 (1994).
[33] K.-P. Kämper, W. Schmitt, and G. Güntherodt, Phys. Rev. B **42**, 10696 (1990).
[34] H.A. Mook, Phys. Rev. **148**, 495 (1966).
[35] R. Raue, H. Hopster, and R. Clanberg, Phys. Rev. Lett. **50**, 1623 (1983).
[36] C.S. Wang and J. Callaway, Phys. Rev. B **15**, 298 (1977).
[37] E.P. Wohlfahrt in *Handbook of Magnetic Materials* **1**, ed. by E.P. Wohlfarth (North Holland, Amsterdam, 1980).
[38] D.C. Tsui, Phys. Rev. **164**, 561 (1967).
[39] O. Jepsen, J. Madsen, and O.K. Andersen, Phys. Rev. B **26**, 2790 (1982).
[40] J.F. Cooke, J.W. Lynn, and H.L. Davis, Phys. Rev. B **21**, 4118 (1980).
[41] A. Liebsch, Phys. Rev. B **23**, 5203 (1981).
[42] J. Bünemann, F. Gebhard, and W. Weber, in preparation.
[43] P. Heimann, F.J. Himpsel, and D.E. Eastman, Solid State Comm. **39**, 219 (1981).
[44] F.J. Himpsel, J.A. Knapp, and D.E. Eastman, Phys. Rev. B **19**, 2919 (1979).
[45] A. Messiah, *Quantum Mechanics*, 3rd printing (North Holland, Amsterdam, 1965).
[46] R.P. Feynman, *Statistical Mechanics*, Frontiers in Physics **36** (Benjamin, Reading, 1972).
[47] R.D. Lowde and C.G. Windsor, Adv. Phys. **19**, 813 (1970).
[48] See, e.g., S.V. Halilov, H. Eschrig, A.Y. Perlov, and P.M. Oppeneer, Phys. Rev. B **58**, 293 (1998).
[49] K. Chen, A.M. Ferrenberg, and D.P. Landau, Phys. Rev. B **48**, 3249 (1993).